Acta Scientiarum
http://periodicos.uem.br/ojs/acta
ISSN on-line: 1807-8664
Doi: 10.4025/actascitechnol.v42i1.44212

Analysis of reinforced concrete beams strengthened with different CFRP lengths

Ricardo José Carvalho Silva[1*], Antônio Eduardo Bezerra Cabral[2], Francisco Eudázio Suriano da Silva Júnior[3], José Leonézio Lopes de Vasconcelos Filho[1] and David Ermerson Farias Eugênio[1]

[1]Universidade Estadual Vale do Acaraú, Avenida da Universidade, 850, 62040-370, Sobral, Ceará, Brazil. [2]Universidade Federal do Ceará, Fortaleza, Ceará, Brazil. [3]Universidade Federal do Rio Grande, Rio Grande, Rio Grande do Sul, Brazil. *Author for correspondence. E-mail: ricardo.carvalho222@gmail.com

ABSTRACT. The application of carbon fiber reinforced polymers (CFRP) as method of strengthening for concrete structures is replacing the conventional strengthening through the bonding of steel plates. However, since it is a recent technique, several codes from different countries still do not consider this type of strengthening. In this work, seven reinforced concrete beams were tested and analyzed. One was used as a reference beam and six were strengthened through the application of CFRP, with some variations regarding the strengthening, with the aim of verifying the efficiency of each system compared to the reference beam. For the computational analysis, the software ANSYS was used along with the plugin ACP (ANSYS Composite PrepPost), by comparing the results obtained in the simulation of the experimental results. Through the laboratory tests and the finite element simulation, it was concluded that the strengthening was efficient in all situations, but it was less efficient in cases where the strengthening was extended to the regions of simple flexure without proper anchorage. It was also possible to notice that the behavior of the simulated beams properly represented the reality, with the beams behaving comparably to the beams of the experimental test.

Keywords: strengthening; carbon fiber; experimental tests; ANSYS.

Received on August 21, 2018.
Accepted on May 10, 2019

Introduction

Due to the wide and increasing use of reinforced concrete structures, it has become common the need to strengthen and repair concrete beams. A strengthening can be used when a bad dimensioning of the structure, pathological manifestations occur, or due to alterations in the use of an edification (due to its high cost of demolishing and making a reinforced concrete structure again).

Strengthening a structure consists in providing a bigger resistance capacity to it and/or recovering its initial physical characteristics of project. According to Hollaway and Teng (2008), this attitude is justified basically when changes in its use occur or when the structure presents any danger to its users due to pathologies or degradations which affect its performance. This way, the use of fiber reinforced polymers (FRP) as method of strengthening for concrete structures has been emphasized, because it is a technique which tend to be widely used, since it is a nondestructive (most of the times), efficient and easy-to-apply method of strengthening.

According to Machado and Machado (2015), the FRP are anisotropic and heterogeneous materials with linear elastic behavior until its failure, their advantage is to be light, resistant to corrosion, have excellent mechanical properties, they easily adapt to any surface and do not need special tools for its application. Currently, the most used FRP are the carbon fiber reinforced polymers (CFRP), which have replaced the strengthening with steel plates because of the previously mentioned favorable characteristics.

However, it is necessary to better study the behavior of reinforced concrete structures strengthened with CFRP, since it is a recent strengthening technique. Brazil and several other countries still do not arrange codes that regulate their use, and the researches that are based on practical experiments about this subject are scarce. Thus, experimental laboratory tests followed by computational simulations by means of numerical modeling become a relevant point of study.

The American standard ACI 440.2R-17 (American Concrete Institute [ACI], 2017) mentions five flexural failure modes in a strengthened reinforced concrete element: a) crushing of the concrete before yielding of

the steel; b) yielding of the steel in tension followed by rupture of the FRP laminate; c) yield of the steel in tension followed by concrete crushing; d) shear/tension delamination of the concrete cover; and e) debonding of the FRP from the concrete substrate (FRP debonding).

Still according to ACI 440.2R-17 (ACI, 2017), the strengthening should be designed so that the governing failure mode does not occur due to delamination of the concrete cover or delamination of the FRP from the concrete substrate. One way to prevent these failure modes is to use lateral anchorage systems such as U-wraps, mechanical fasteners, fiber anchors or U-anchors, which have been proven successful at delaying or even preventing debonding failure of the longitudinal FRP.

Thus, the aim of this work is to investigate, through the experimental analysis and computational simulations, the efficiency of the system of strengthening CFRP in reinforced concrete beams submitted to flexure. Seven reinforced concrete beams with the same reinforcements were tested and computationally simulated, but with some differences in relation to the positioning of the strengthening, in a way it was possible to observe the alterations in the behavior of each beam. One of the beams was not strengthened; it was a beam of reference.

The investigation of beams with strengthening of short length, anchored only in the region of simple flexure, was motivated to compare with the beams with strengthening of long-length, anchored in the region of simple flexure, whose negative point is the possibility of rupture by detachment of the fiber, caused by the shear stresses. Besides that, the ACI 440.2R-17 (ACI, 2017). Besides that, the ACI 440.2R-17 (ACI, 2017) recommendation on the use of anchorage at the lateral faces of the beams (U-anchors), to avoid rupture by detachment of the strengthening, also motivated this study.

Chen, Pham, Sichembe, Chen, and Hao (2018) explain that the U-anchors increase the capacity of the composite that is used, that is, increase the use of the elongation strain capacity, leading to higher ductility. D'Antino and Triantafillou (2016) analyzed the accuracy of analytical models widely used in order to evaluate the flexural and shear contributions provided by the FRP. The authors observed that some formulations still need to be refined, which may be due to results available in the literature regarding U-anchors being not very conclusive.

This research was divided into two stages: experimental and computational. In the experimental stage, the tests of the beams were performed at the laboratory of Nutec (Industrial Nucleus Technology Foundation of Ceara State). In this stage, the tests of characterization of the properties of the concrete and the experimental tests of beams were included. In the computational stage, the same beams were modeled and computationally simulated through the finite element software ANSYS, in a nonlinear way. In the end, there were discussions by comparing the results, and then, the conclusions were elaborated.

Material and methods

Experimental program

Seven reinforced concrete beams were made and tested, which had the same reinforcements. All the beams were molded in forms of plasticized wood. They were concreted and densified with vibrator. For a week, four times a day, the wet curing was done on the beams using a blanket to retain moisture. The concrete mix used was as follows: cement = 50 kg, coarse sand = 0.09, gravel (granite) = 0.10 and water = 0.03 m^3.

The first beam (V1) was a beam of reference, with no strengthening. The other beams were differently strengthened with CFRP. The beams were designed so that their failure would occur due to flexure, since the strengthening was introduced to enhance the flexural resistance. Figure 1 shows the dimensions, the detailing of the reinforcements and the strengthenings of the strengthened beams V2, V3, V4, V5, V6 and V7.

In spite of the fact that the analyzed beams presented reduced dimensions in comparison to the majority of the real beams, it is necessary to emphasize that it was not the purpose of this work to determine any correlation between the reduced model and prototype through the Dimensional Analysis and Laws of Similarity. The aim was to compare the structural behavior of the strengthened beams to the beam of reference.

The experimental test consisted of the traditional Stuttgart test (or four points test), as shown on Figure 2.

The load was applied in a gradual and increasing way, from top to bottom, through a manual hydraulic jack and registered by means of a load cell. As it can be noticed on Figure 2, three Linear Variable Displacement Transformer (LVDT) were placed in angles glued to the beam in order to measure the displacements in the middle of the span of the beam and in the points of the loads of reaction.

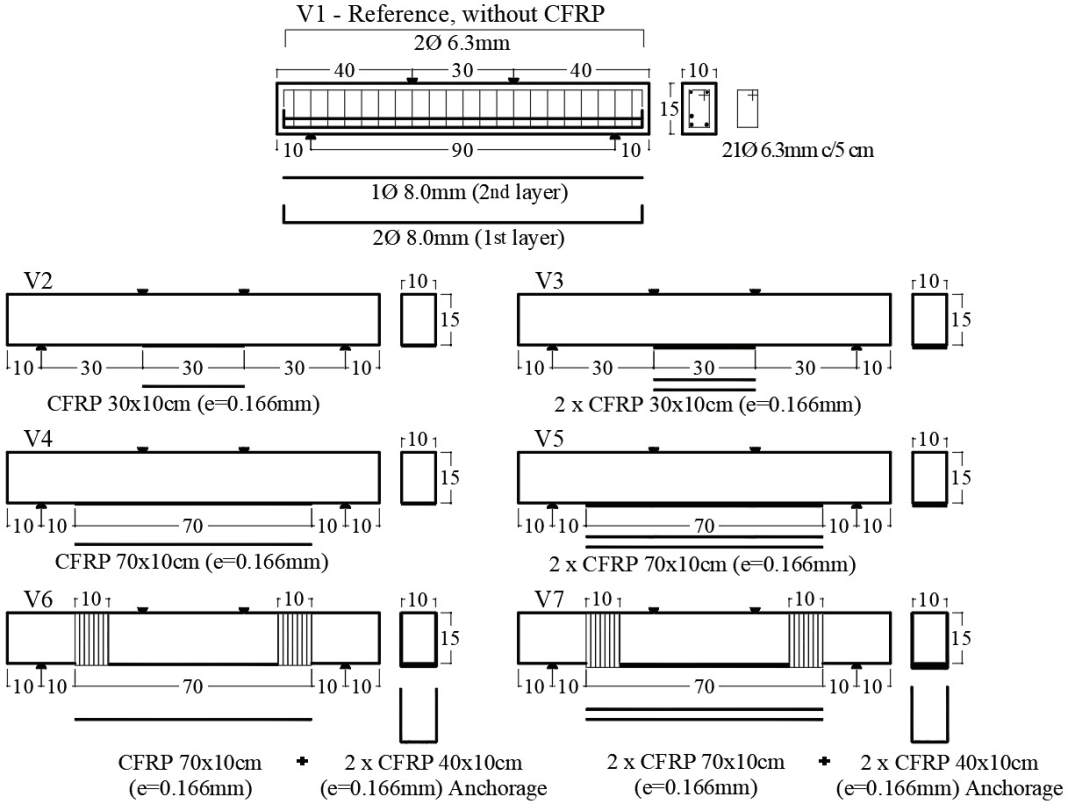

Figure 1. General detailing of the tested beams, where 'e' = thickness. Source: Author.

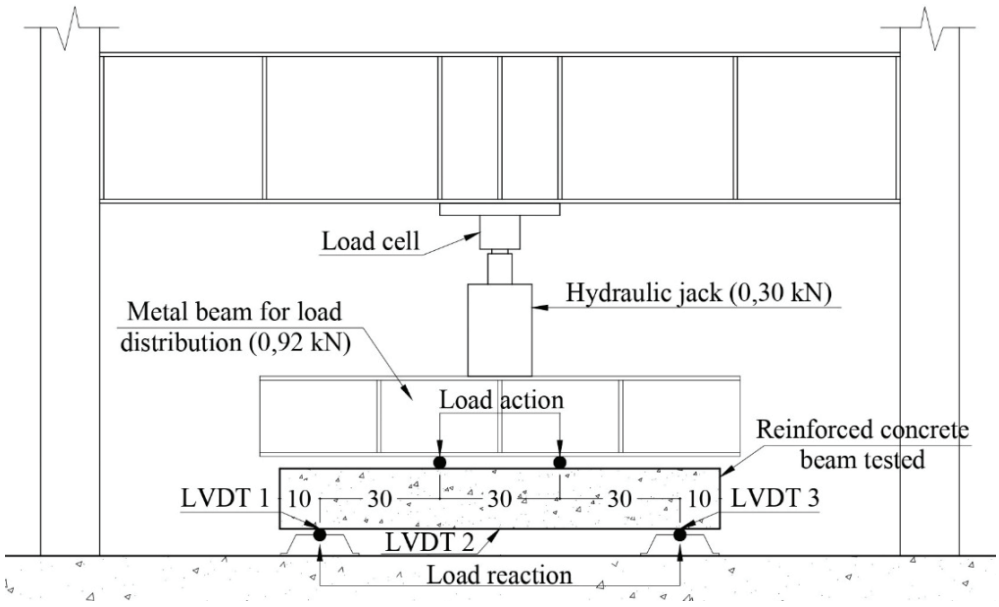

Figure 2. Scheme of the test for the tested beams. Source: Author.

The loads and displacements of the tested beams were monitored by a computer linked to the system of acquisition of data along with the LVDTs. During the application of the loads, each increment of 10 kN, the test was interrupted in order to mark the visible cracks in the beams. This procedure was followed for all beams up to their failure.

Computational simulation

Finite element software ANSYS Workbench (student version) and its tool ANSYS Composite PrepPost (ACP) were used in order to simulate the studied beams to validate the experimental test. Besides the reinforced concrete, it also aimed to simulate the strengthening of carbon fiber and the direction of its fibers according to the project of the tested beams.

Only half of each beam was modeled and it was defined a plan of symmetry. According to Lee (2014), the tool of symmetry of ANSYS considers that the displacement out of the plan of symmetry and the rotation on the plan of symmetry are null. This way, the computational workload and the time of the analysis could be reduced without interfering the trustworthiness of the results.

In order to represent the reinforced concrete, the combination of two finite elements of ANSYS was used: the three-dimensional solid element Solid65 for the concrete and the three-dimensional linear element Link180 to represent the steel. A limitation of the element Solid65 is that it is compatible only with the discrete and the smeared modeling; it is not compatible with the embedded reinforcement. For the discrete modelling, it is necessary that the nodes of the beam elements match with the nodes of the reinforcement, which increases the number of finite elements in the mesh, according to Figure 3. However, this combination is widely used to simulate reinforced concrete, as in the cases of Hossain, Karim, Islam, and Zain (2014), because Solid65 is the default element with a formulation for concrete in the ANSYS software, which uses the Willam-Warnke failure criterion.

In order to simulate the CFRP, the element Shell281 was used through the tool ACP, to synthesize layers of composite materials and to define the directions of the fibers for analyses of finite elements in ANSYS (ANSYS, 2013a).

A mesh without midside nodes of 25 mm was used for the Solid65 (concrete) and Link180 (steel rebar). Thus, the nodes of the elements of the concrete could correspond exactly with the nodes of the elements of the steel (longitudinal bars and stirrups). The nodes that matched were bound through the command Ceintf, which shares the stresses involved between the nodes of the selected elements through the creation of equations of restriction (ANSYS, 2013b). Table 1 lists the properties defined in the simulation for the concrete and for the steel, by taking into account the tests performed in the specimens of concrete and the specifications of the manufacturer for the steel.

The values for the ultimate strengths of concrete were obtained through experimental tests of cylindrical specimens. The elasticity modulus was calculated according to the recommendations of the ABNT NBR 6118 (*Associação Brasileira de Normas Técnicas* [ABNT], 2014). The values for the shear transfer coefficients are between ranges widely used in the literature, as in Belal, Mohamed, and Morad (2015).

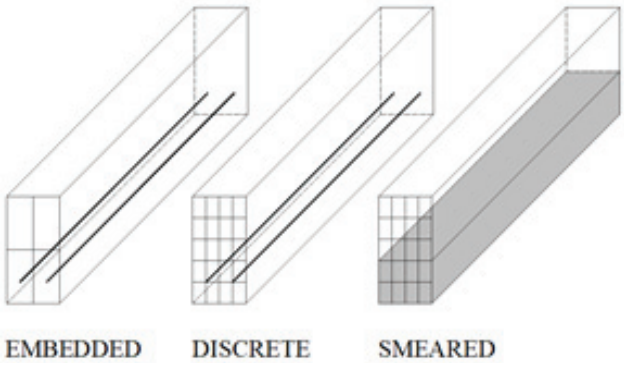

Figure 3. Types of modelling of the reinforcements. Source: Author.

Table 1. Properties for the concrete and the steel.

Concrete	Value
Modulus of initial elasticity (E_{ci})	30.56 GPa
Poisson's ratio (υ_c)	0.20
Shear transfer coefficient (open cracks)	0.35
Shear transfer coefficient (closed cracks)	1.00
Uniaxial compressive strength (f_c)	30.64 MPa
Uniaxial tensile strength ($f_{ct,m}$)	3.20 MPa
Steel	Value
Modulus of elasticity (E_s)	210.00 GPa
Poisson's ratio (υ_s)	0.30
Yield strength (f_{yk})	500.00 MPa
Tangent modulus (E_T)	20.00 MPa
Steel area for ø = 6.3 mm	31.17 mm²
Steel area for ø = 8.0 mm	50.27 mm²

Source: Author.

Due to the lack of experimental data for the mechanical properties of the steel and CFRP, it was used in the analyses the values provided by the manufacturers. These values were considered reliable and should not affect the precision of the simulations.

In order to provide plastic characteristics to the concrete (Solid65) in the simulation, it was defined a multilinear stress-strain graph for compression through the command MISO (multilinear isotropic hardening). The points of this graph were obtained from Equation 1, based on the average resistance obtained from the results of the tests of the specimens of concrete.

$$\sigma_c = f_{c,m}\left[1 - \left(1 - \frac{\varepsilon_c}{\varepsilon_{c2}}\right)^n\right] \quad (1)$$

where:

σ_c : compressive strength of the concrete;

$f_{c,m}$: average compressive strength of the concrete;

ε_c : strain of the concrete;

ε_{c2} : strain of the concrete in the beginning of the yield plateau;

n : exponent (2 for concretes under 50 MPa).

In order to avoid problems of convergence, the reduction of stress of the concrete after ε_c = 2‰ was ignored. The adopted graph was similar to the ones specified by the codes NBR 6118 (ABNT, 2014) and Model Code (International Federation for Structural Concrete [FIB], 2010). Thus, the graph effectively used for the concrete is shown on Figure 4.

As a standard procedure in a Solid65 analysis, the tensioned region of the concrete was considered an isotropic material with softening. That is, before cracking occurs, the material behaves in a linear-elastic way. After cracking, it can be considered a contribution model of the concrete among cracks.

For the steel, it was defined a bilinear stress-strain graph through the command BISO (bilinear isotropic hardening). It was defined a small inclination in the graph after the material yields, with 20 MPa tangent modulus, which helps to avoid loss of stability after the yield occurs.

For the CFRP, it was used a 12.5 mm mesh with midside nodes and the contacts were defined as bonded with the formulation MPC (multi-point constraint), where it is not allowed to occur separation or slipping between the faces and equations of restriction are inserted between the contacting elements. The carbon fibers followed the same directions of the fibers that were tested at the laboratory. Their physical and mechanical properties were defined according to the specifications of the manufacturer for the fiber used in the experimental tests (model CFW300 by Viapol). Table 2 lists the properties defined for the CFRP in the computational simulation.

The computational test of the beams occurred by the application of the load from top to bottom. For the point of application of load, a semi-cylindrical solid similar to the one used at the laboratory was modeled. As for the point of reaction, the displacement in the direction of the Y axis of the nodes was disallowed. The beams are shown on Figure 5.

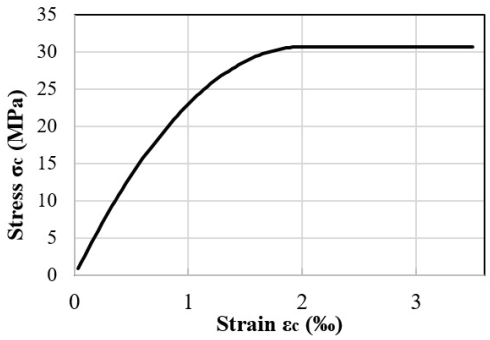

Figure 4. Stress-strain graph of the concrete for the simulation. Source: Author.

Table 2. Properties of the CFRP.

Property	Value
Type of mantle	Unidirectional
Modulus of elasticity (E_f)	230.00 GPa
Tensile strength (f_{fu})	4900.00 MPa
Maximum strain (ε_{fu})	2.10%
Thickness (e)	0.166 mm

Source: Author.

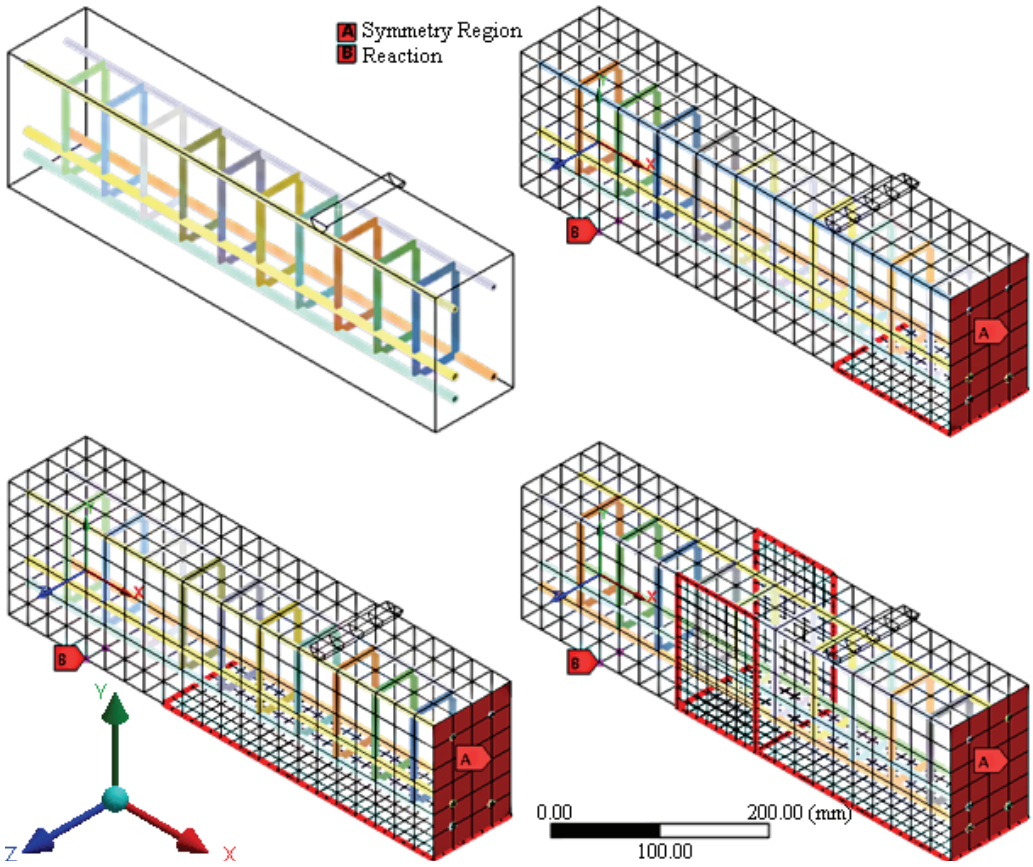

Figure 5. Aspect of the beams for the computational simulation. Source: Author.

For this nonlinear analysis, one load step and 250 substeps were defined. It was considered that the load of failure of the simulated beams would be the one that surpassed the strength of the beam. When an excessive load is applied and it exceeds the limits of resistance of the beam, ANSYS interrupts the simulation and shows an error that indicates excessive loading. Thus, in order to determine the ultimate load, several attempts were made until ANSYS showed the error of excessive load. Then, the results were refined until a precision of 2 N was achieved.

Results and discussion

In the end, with the aim of determining the average resistances to compression and to tension of the concrete used in the beams, six cylindrical specimens of 10x20 cm made on the same day and with the same concrete used in the manufacturing of the beams, were tested. Three of them were submitted to the standard axial compression test, and the other three were submitted to the diametrical compression test through the method known as Brazilian Test. The tests in the specimens were performed on the same day of the test of the beams. Table 3 shows the resistances achieved by the concrete in each specimen.

The loads of failure of the tested experimental beams $P_{u,exp}$ are shown on Table 4, where it is also shown the increase of resistance δ which the CFRP provided to the strengthened beams in comparison to the beam of reference (V1). It is still presented the way of failure and the estimated loads of flexural failure according to the codes ACI 440.2R-17 (American Concrete Institute [ACI], 2017) and ACI 318M-14 (ACI, 2014). In addition, the estimated loads of failure by Detachment of the fiber, following the recommendations of CNR-DT 200 (National Research Council [CNR], 2013), are also presented.

Figure 6 shows the pictures of the tested beams after the failure. It is worth reminding that, each 10 kN of load, the visible cracks and their correspondent loads were marked with a marker.

In all cases, the strengthening was able to increase the resistances of the tested beams. In the case of beam V2, the fiber applied only in the zone of pure flexure increased 38.45% of resistance in comparison to the beam of reference (V1). As for V3, strengthened with an additional layer of CFRP in comparison to V2, it presented a gain of resistance of 9.24% in comparison to V2 and 51.25% in comparison to V1. However, the increase of the length of the applied fiber did not mean an increase in the resistance of the beams V4 and V5

in relation to the beams V2 and V3. Instead of that, the increase in the amount of fiber caused the decrease of the load of failure of V4 in 18.26% in comparison to beam V2, whereas the load of failure of V5 was decreased in 24.93% in comparison to V3. It occurred because of the detachment of the superficial concrete layer in contact with the epoxy adhesive in the zone of simple flexure, where there is presence of shear stress, just as Hollaway and Teng (2008) emphasize in their work. However, it should be mentioned that a distance of 10 cm was left between the end of the fibers and the axis of the support, so that there was no risk that the fibers tore through the contact with the support. In conventional structures, the ACI 440.2R-17 (ACI, 2017) recommends that the anchorage is made respecting a L_{df} length counted after the crack bending moment. This L_{df} anchorage length for the beams V4 and V5 would be 8.3 cm and 11.7 cm, respectively.

This can be confirmed by the test of the beams V6 and V7, which, besides being strengthened in the zone of simple flexure, as in the beam V4, they were also anchored in this region, in order to prevent the detachment of the superficial layer of concrete, as recommends the ACI 440.2R-17 (ACI, 2017). Because of that, beams V6 and V7 had their resistances increased in 84.36 and 93.00%, respectively, in comparison to beam V1.

It can be noticed that the use of CFRP only in the middle region, like in V2 and V3, reduced the process of cracking of the concrete in the zone of pure flexure, even though, this is the region of maximum bending moment.

In beams V4 and V5, the anchorage of the strengthening in the zone of simple flexure turned to be a point of fragility, since the presence of shear stresses influenced in the detachment of the strengthening, making it less efficient. On the other hand, in beams V6 and V7, the use of strengthening in the zones of pure and simple flexure along with the anchorage in the sides of the beams increased the resistance of the beams without preventing the appearance of cracks, which was an important factor for the ductility of the beam.

The load-deflection graph is shown on Figure 7. It can be observed that, in spite of having increased the load of failure, the CFRP reduced the displacement and the ductility of the majority of the strengthened beams, mainly in the case of beams V4 and V5, which achieved the load of failure with only 4.19 mm and 3.44 mm of deflection, respectively, against 9.56 mm in the beam of reference (V1). That is, besides of the fact that it did not increase the ultimate load very much, the detachment of the CFRP in beams V4 and V5 also reduced the displacement, making them beams with fragile behavior and unexpected failure, because there is basically no yield plateau.

About beam V2, in spite of the increase in the ultimate load, the displacement was reduced in 33.41% in comparison to beam V1, but the application of one more layer of strengthening (on beam V3) provided, besides resistance, bigger ductility in comparison to beam V2, surpassing the beam of reference. However, by comparing beams V4 and V5, the addition of one more layer of strengthening in the beam did not increase significantly its resistance (2.61%) and resulted in smaller displacement.

Table 3. Result of the tests of the specimens.

Specimen (compression)	f_c (MPa)	$f_{c,m}$ (MPa)
CPI	27.61	
CPII	32.40	30.64
CPIII	31.91	
Specimen (tension)	f_{ct} (MPa)	$f_{ct,m}$ (MPa)
CPIV	3.01	
CPV	3.02	3.20
CPVI	3.58	

Source: Author.

Table 4. Loads of failure of the experimental test.

Beam	Strengthening	$P_{u,exp}$ (kN)	δ (%)	Flexure $P_{u,Flexure,ACI}$ (kN)	Detachment $P_{u,detachment,CNR}$ (kN)	Type of Failure
V1	-	48.14	-	51.88	-	Flexure
V2	FP[1]	66.65	38.45	-	-	Flexure
V3	FP[1] DL[4]	74.00	53.72	-	-	Flexure
V4	FPS[2]	54.48	13.17	-	43.78	Detachment of the fiber
V5	FPS[2] DL[4]	55.90	16.12	-	48.00	Detachment of the fiber
V6	FPS+A[3]	88.75	84.36	77.82	-	Flexure
V7	FPS+A[3] DL[4]	92.91	93.00	84.37	-	Flexure

[1]FP: strengthening in the zone of 'pure flexure'; [2]FPS: strengthening in the zones of 'pure and simple flexure'; [3]FPS+A: strengthening in the zones of' pure and simple flexure + anchorage in the zone of simple flexure'; [4]DL: 'double layer'. Source: Author.

Figure 6. Beams after failure. Source: Author.

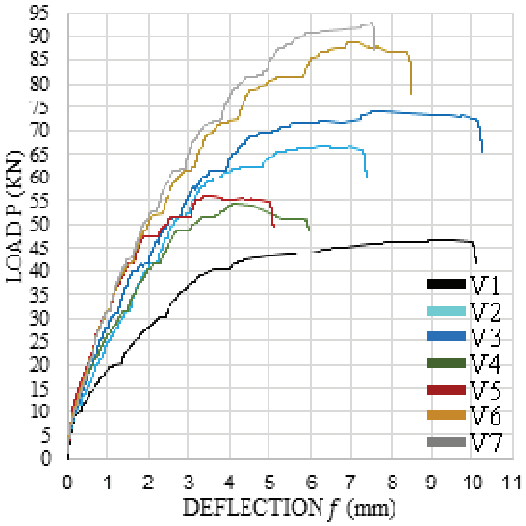

Figure 7. Load-deflection graph of the tests. Source: Author.

Beams V6 and V7 obtained the best performances when it comes to the ultimate resistance, but with losses of displacements of 15.95 and 25.14%, respectively. Like beams V4 and V5, the double strengthening of CFRP in V7 increased its ultimate resistance in comparison to V6 (4.69%), but it damaged the displacement in comparison to the same beam (10.93%).

About the computational test, Table 5 presents the loads of failure $P_{u,com}$, the increase of resistance δ_{com} which the CFRP provided (in comparison to beam V1) and the loads of failure calculated according to ACI ($P_{u,ACI}$).

The ultimate loads of the computational test achieved values close to the results obtained by the experimental test. The biggest variations in comparison to the experiment were in beams V4 and V5. It can be explained due to the fact that these two beams suffered failure by the detachment of the fiber in the

experimental test, what did not occur in the computational simulation because the adherence between the materials was considered perfect. However, in a general way, the results were similar and coherent. Besides that, the loads of failure obtained in the computational simulation varied similarly to the ones obtained in the experimental test. As in the experimental analysis, the following results were verified:

- V1 was the beam which achieved the smallest resistance;
- The strengthening in the zone of pure flexure improved significantly the performance in beams V2 and V3;
- The increase of the amount of strengthening for the zone of simple flexure decreased the performance of beams V4 and V5 in comparison to beams V2 and V3;
- Beam V7 was the one that obtained the greatest load of failure;
- Beams with two layers of CFRP had better performance than the beams with only one layer.

The loads of failure of the simulation were close to the theoretical loads calculated by the ACI method. Figure 8 shows the behavior of the simulated beams through the relation the load *P* and the displacement *f* in the middle of the span. It is important to emphasize that, in the graph of Figure 8, it was not possible to show the strain softening zone in the end of the graph, when the load of failure is achieved. It occurred because in these simulations, forces were applied instead of displacements, and ANSYS stopped the simulation when the ultimate load was achieved. For the same reason, it can be noticed that the beam of reference had little deflection when compared to V1 of the experiment.

The computationally simulated beams behaved similarly to the ones tested at the laboratory. The graph produced by the computational simulation returned coherent and reliable values.

Table 5. Loads of failure of the computational simulation.

Beam	Strengthening	$P_{u,com}$ (kN)	δ_{com} (%)	$P_{u,ACI}$ (kN)
V1	-	51.99	-	51.88
V2	FP[1]	65.91	26.77	-
V3	FP[1] DL[4]	68.79	32.31	-
V4	FPS[2]	63.43	22.00	-
V5	FPS[2] DL[4]	66.94	28.74	-
V6	FPS+A[3]	75.50	45.22	77.82
V7	FPS+A[3] DL[4]	77.84	49.72	84.37

[1]FP: strengthening in the zone of 'pure flexure'; [2]FPS: strengthening in the zones of 'pure and simple flexure'; [3]FPS+A: strengthening in the zones of 'pure and simple flexure + anchorage in the zone of simple flexure'; [4]DL: 'double layer'. Source: Author.

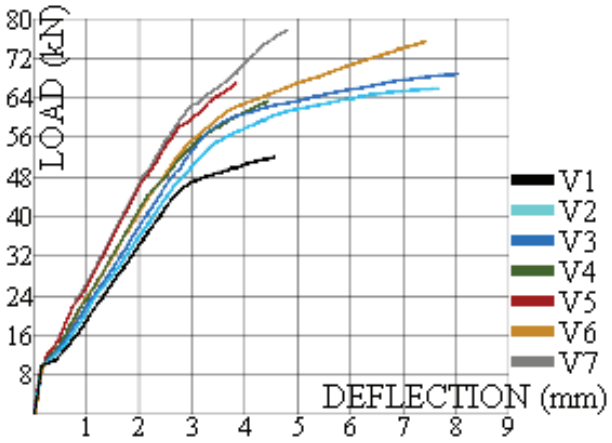

Figure 8. Load-deflection graph of the beams in the computational analysis. Source: Author.

Conclusion

The CFRP, as strengthening in reinforced concrete beams has shown to be very efficient, but it is necessary to understand well the mechanics involved in the loading of a beam and to be careful when applying this type of strengthening in regions with shear stresses. Thus, in order to provide safety, the application of CFRP in zones of simple flexure without the appropriate anchorage of this strengthening in the lateral faces of the beam should be avoided.

The anchorage in the lateral faces of the beams (V6 and V7) has shown to be an efficient measure against the detachment of the fiber in order to avoid the fragile failure, allowing the beams with this type of strengthening to achieve higher loads of failure. Besides that, the anchorage of the fiber in the lateral faces of the beams, in the zone of simple flexure, did not prevent the appearance of cracks before the failure and allowed the beams to undergo considerable displacements**,** which contributed for the maintenance of the ductility.

Regarding the results of the computational simulation, the results, in general, confirmed and gave more reliability to the experimental values.

It is important to emphasize that the conclusions of this work are restricted only to the results of the tests presented. Thus, it is suggested that more tests of beams, with and without strengthening, are performed with the aim of better validating this work.

Acknowledgements

The authors would like to thank Viapol for the supply of materials used and the Federal University of Ceará (UFC) together with Nutec for their support of experimental tests in this research.

References

American Concrete Institute [ACI]. (2014). *ACI 318M-14: building code requirements for structural concrete and commentary.* Farmington Hills, MI: ACI. doi: 10.14359/51688187

American Concrete Institute [ACI]. (2017). *ACI 440.2R-17: guide for the design and construction of externally bonded frp systems for strengthening concrete structures.* Farmington Hills, MI: ACI.

ANSYS Inc. (2013a). *ANSYS composite preppost user's guide [Manual], Release 15.0*. Canonsburg, PA: ANSYS Inc.

ANSYS Inc. (2013b). *ANSYS mechanical APDL material reference [Manual], Release 15.0*. Canonsburg, PA: ANSYS Inc.

Associação Brasileira de Normas Técnicas [ABNT]. (2014). *NBR 6118: design of concrete structures – procedure*. Rio de Janeiro, RJ: ABNT.

Belal, M. F., Mohamed, H. M., & Morad, S. A. (2015). Behavior of reinforced concrete columns strengthened by steel jacket. *HBRC Journal, 11*(2), 201-212. doi: 10.1016/j.hbrcj.2014.05.002

Chen, W., Pham, T. M., Sichembe, H., Chen, L., & Hao, H. (2018). Experimental study of flexural behaviour of RC beams strengthened by longitudinal and U-shaped basalt FRP sheet. *Composites Part B: Engineering, 134*, 114-126. doi: 10.1016/j.compositesb.2017.09.053

D'Antino, T., & Triantafillou, T. C. (2016). Accuracy of design□oriented formulations for evaluating the flexural and shear capacities of FRP□strengthened RC beams. *Structural Concrete, 17*(3), 425-442. doi: 10.1002/suco.201500066

Hollaway, L. C., & Teng, J. G. (2008). *Strengthening and rehabilitation of civil infrastructures using fibre-reinforced polymer (FRP) composites*. Boca Raton, FL: Woodhead Publishing Limited. doi: 10.1201/9781439832448

Hossain, M. M., Karin, M. R., Islam M. A., & Zain, M. F. M. (2014). Crack chronology of reinforced concrete beam under impact loading. *International Digital Organization for Scientific Information*, *Middle-East Journal of Scientific Research, 21*(9), 1663-1669. doi: 10.5829/idosi.mejsr.2014.21.09.913

International Federation for Structural Concrete [FIB]. (2010). *Model code 2010.* Lausanne, CH: FIB.

Lee, H. (2014). *Finite element simulations with ansys workbench*. Mission, KS: SDC Publications.

Machado, A. P., & Machado, B. A. (2015). *Reforço de estruturas de concreto armado com sistemas compostos FRP: teoria & prática*. São Paulo, SP: Pini.

National Research Council [CNR]. (2013). *CNR-DT 200/2012: advisory committee on technical recommendations for construction. Guide for the design and construction of externally bonded FRP systems for strengthening existing structures*. Rome, IT: CNR.